



Cite this: *Org. Biomol. Chem.*, 2024, **22**, 1812

Clemastine/tamoxifen hybrids as easily accessible antileishmanial drug leads[†]

V. S. Agostino, ^{a,d} M. L. Buerdsell, ^a S. R. B. Uliana, ^b P. W. Denny, ^c A. C. Coelho ^d and P. G. Steel ^{*,a}

A library of hybrid molecules is developed based on the common chemical features shared by clemastine and tamoxifen both of which are well known for their antileishmanial activities. In the initial screening against *Leishmania major* and *L. amazonensis* promastigotes, as well as cytotoxicity assays using HepG2 cells, several hybrids showed submicromolar activity against the parasite and no toxicity against human cells. The compounds with an $EC_{50} < 2 \mu\text{M}$ against promastigotes of both species and a selectivity index >10 were further characterized against intracellular amastigotes as well as promastigotes of species that cause both visceral and cutaneous leishmaniasis, such as *L. infantum* and *L. braziliensis*, respectively. These sequential screenings revealed the high pan-activity of this class of molecules against these species, with several compounds displaying an $EC_{50} \leq 2 \mu\text{M}$ against both promastigotes and intracellular amastigotes. Two of them were identified as the potential templates for lead optimization of this series having shown the highest activities against all species in both stages of parasite. The present findings can serve as a good starting point in the search for novel antileishmanial compounds that are easy to access and highly active.

Received 22nd December 2023,
Accepted 30th January 2024

DOI: 10.1039/d3ob02091f

rsc.li/obc

1. Introduction

Leishmaniasis is a group of vector-borne neglected tropical diseases caused by approximately 20 species of the parasite of the genus *Leishmania*.¹ According to the World Health Organization (WHO), more than one billion people are at risk of infection in over 90 countries where the leishmaniasis are endemic with major implications for economic viability, demonstrated by the 1.6 million DALYs (disability-adjusted life years) lost due to the disease.² The leishmaniasis are caused by approximately 20 different parasite species leading to different clinical manifestations ranging from lesions in the skin to highly disfiguring destruction of facial mucosa and potentially lethal infections in the liver, spleen, and bone-marrow.^{3–5} The actual impact of the disease is challenged by limitation on diagnosis and the number of cases that are under reported. However, recent estimates by WHO suggest that there are at least 300 000 new cases of visceral leishmaniasis (VL) leading approximately 20 000 deaths each year.^{6,7} Cutaneous leishmaniasis (CL) is more prevalent with over

1 million new annual cases.⁷ Although generally non-fatal, CL is often associated with other potentially lethal secondary infections, as well as a social stigma that is correlated with longer term mental health issues leading to a collective adverse impact to over 40 million people worldwide.^{8–10} This situation is compounded by the fact that the current therapeutic arsenal is limited to a few drugs which have multiple shortcomings including severe side effects, unpleasant modes of administration, high cost, species dependent activity and the emergence of resistant parasites.^{11–13} These issues result in poor patient adherence, impairing the efficacious elimination of the disease. Collectively, this makes the search for new alternative cheap broad-spectrum treatments for leishmaniasis an urgent issue.

The cost of, and time required for, *de novo* drug discovery challenges the development of new chemotherapies and renders the adoption of a drug repurposing strategy attractive.^{14–16} Towards this end, we have previously reported that the breast cancer drug, tamoxifen,^{17,18} and the antihistamine clemastine fumarate¹⁹ have promising activity against several species of *Leishmania*, both *in vitro* and *in vivo*. Tamoxifen is a well-known selective estrogen receptor modulator (SERM) that has been used since the 1970s in the treatment and prevention of estrogen-dependent breast cancer.^{20,21} Even though estrogen receptors have not been identified in *Leishmania*,¹⁷ tamoxifen displayed micromolar activity against intramacrophage amastigotes of *L. braziliensis* ($EC_{50} = 1.9 \mu\text{M}$), *L. amazonensis* ($EC_{50} = 4.5 \mu\text{M}$) and *L. infantum* ($EC_{50} = 2.4 \mu\text{M}$), in addition to also clearing infections *in vivo* in mouse models

^aDepartment of Chemistry, Durham University, UK. E-mail: p.g.steel@durham.ac.uk

^bDepartment of Parasitology, Biomedical Sciences Institute, University of São Paulo, Brazil

^cDepartment of Biosciences, Durham University, UK

^dDepartment of Animal Biology, Institute of Biology, University of Campinas, Brazil

† Electronic supplementary information (ESI) available. See DOI: <https://doi.org/10.1039/d3ob02091f>



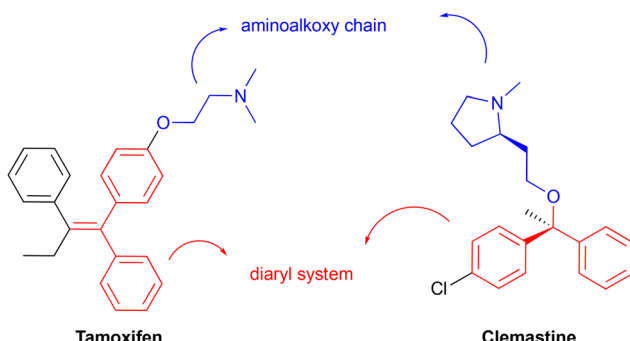


Fig. 1 Clemastine and tamoxifen common structural features, an aminoalkoxy chain (blue) and a diaryl system (red).

of the disease when administered intraperitoneally.^{17,22–25} Clemastine fumarate is a first-generation H1 receptor antagonist²⁶ with sub-micromolar activity against *L. amazonensis* ($EC_{50} = 0.46 \mu\text{M}$), and an *in vivo* efficacy comparable to that obtained with the clinically used meglumine antimoniate (Glucantime®) in a mouse model of *L. amazonensis* infection.¹⁹

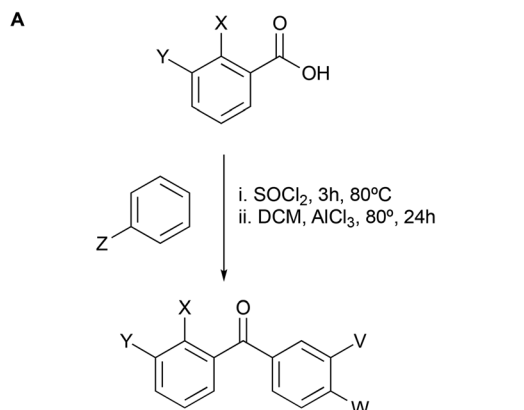
Although both compounds exhibit polypharmacology, they share a common mode of action involving the inhibition of *inositol phosphorylceramide synthase* (IPCS), which is a key enzyme in the sphingolipid biosynthetic pathway of the parasite.^{19,27} Moreover, both share common structural elements, in particular an aminoalkoxy side chain (Fig. 1, head group, blue) and a diarylmethane (Fig. 1, scaffold, red), and it was therefore hypothesised that these features contribute to their common antileishmanial activity. Whilst a number of syntheses have been reported for each compound,^{28,29} both present challenges, particularly in the control of stereochemistry. In this report we describe the synthesis of hybrid compounds that build on this commonality, are simple to access and retain good levels of antileishmanial activity across a broad spectrum of parasite species.

2. Results and discussion

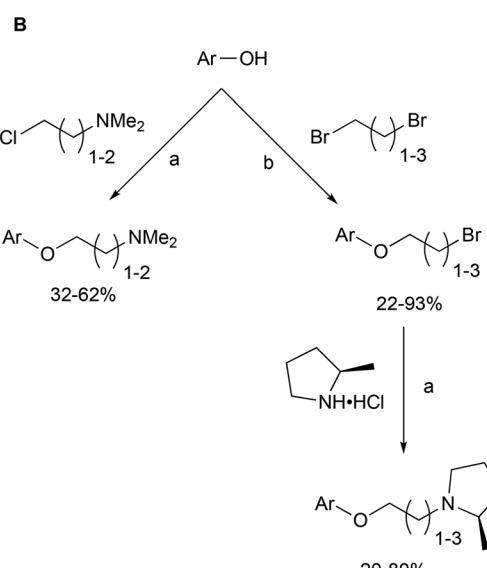
2.1. Design and synthesis of clemastine/tamoxifen hybrid molecules

Combining the diaryl ethene from tamoxifen and the diaryl carbinol from clemastine led to a benzophenone being chosen as the parent scaffold that is both commercially available and chemically accessible, making modifications more approachable. Whilst scaffolds A, B, C, F and H were found commercially, the other scaffolds were synthesized in one-step through a Friedel–Crafts acylation protocol (Scheme 1A). Modifications introduced in this way included varying the position of the aminoalkoxy chain on ring B, as well as the addition of substituents into ring A to explore the essentiality of the clemastine chlorine substituent for activity as well as tolerance to bulkier substituents (Fig. 2).

Each scaffold unit was then combined with two series of headgroups *via* a series of simple S_N2 reactions summarized in



D (X = Cl, Y = H, Z = OMe, V = H, W = OH), 70%
 E (X = H, Y = Cl, Z = OMe, V = H, W = OH), 64%
 H (X = H, Y = OMe, Z = Cl, V = OH, W = H), 87%
 I (X = H, Y = OMe, Z = Me, V = OH, W = H), 83%
 J (X = H, Y = OMe, Z = $\text{CH}_2(\text{CH}_3)_2$, V = OH, W = H), 99%



Scheme 1 Synthesis of tamoxifen/clemastine hybrids. (A) Synthesis of *para*-hydroxybenzophenones D and E and *meta*-hydroxybenzophenones H, I and J. (B) Attachment of headgroups to hydroxybenzophenones. a – Na_2CO_3 , KI, MeCN, 80 °C, 24 h; b – Cs_2CO_3 , MeCN, RT, 24 h.

Scheme 1B. These were the dimethylaminoalkyl motifs present in tamoxifen (Fig. 2L), and the (2*R*)-methyl-*N*-(ω -alkyl)pyrrolidines (Fig. 2M) that we have previously shown to have similar activity to clemastine but with easier chemical accessibility.³⁰

Finally, two more focused set of compounds were prepared in which the benzophenone was replaced by a simple benzoid scaffold (Scheme 2) and systems in which the ketone component was replaced by an oxygen (diphenyl ether) or a carbon (diphenylmethane) (Scheme 3).

2.2. Antileishmanial screening of clemastine/tamoxifen hybrids

A screening workflow was established with the aim of selecting the hybrids with the most promising therapeutic properties



Scaffold

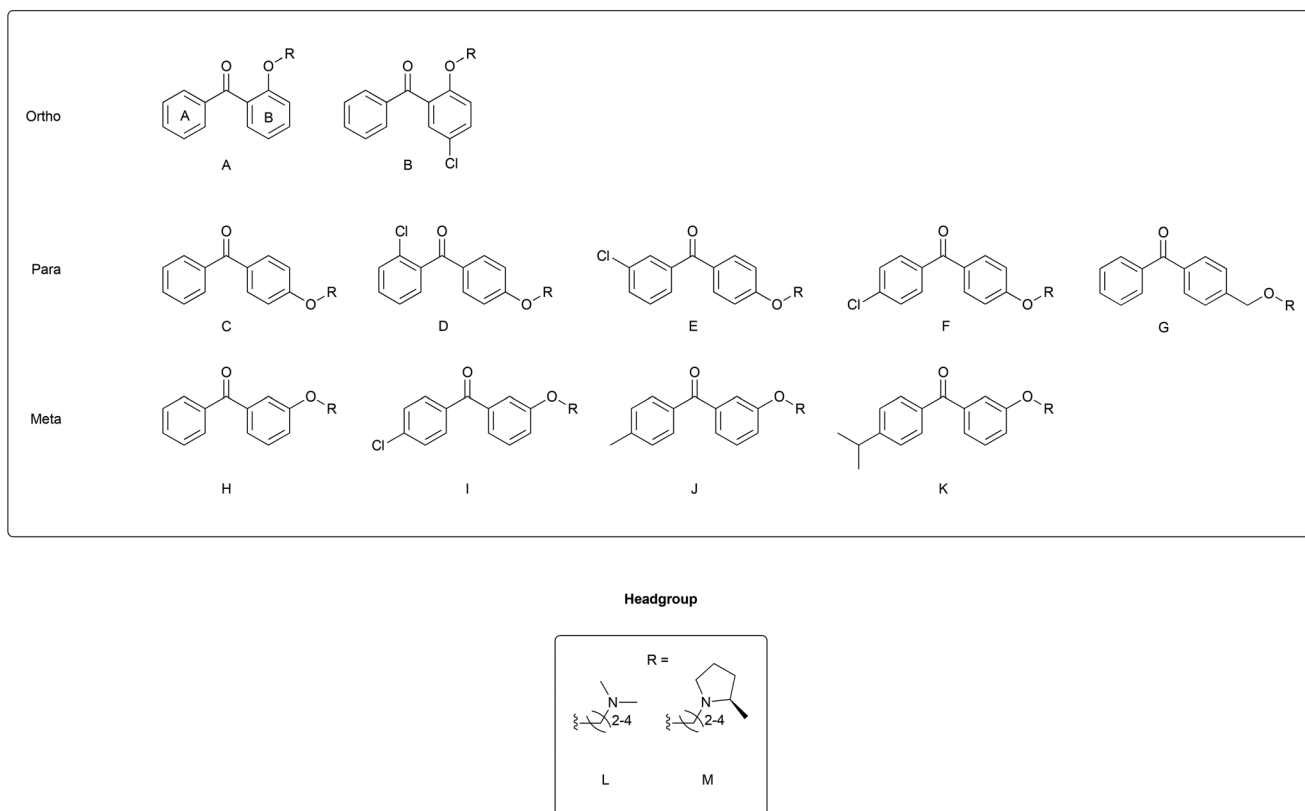
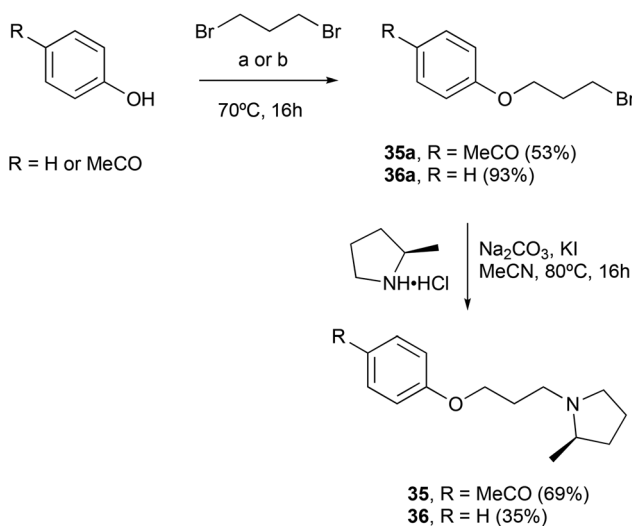


Fig. 2 Benzophenone scaffolds designed for use in the synthesis of clemastine/tamoxifen hybrids.



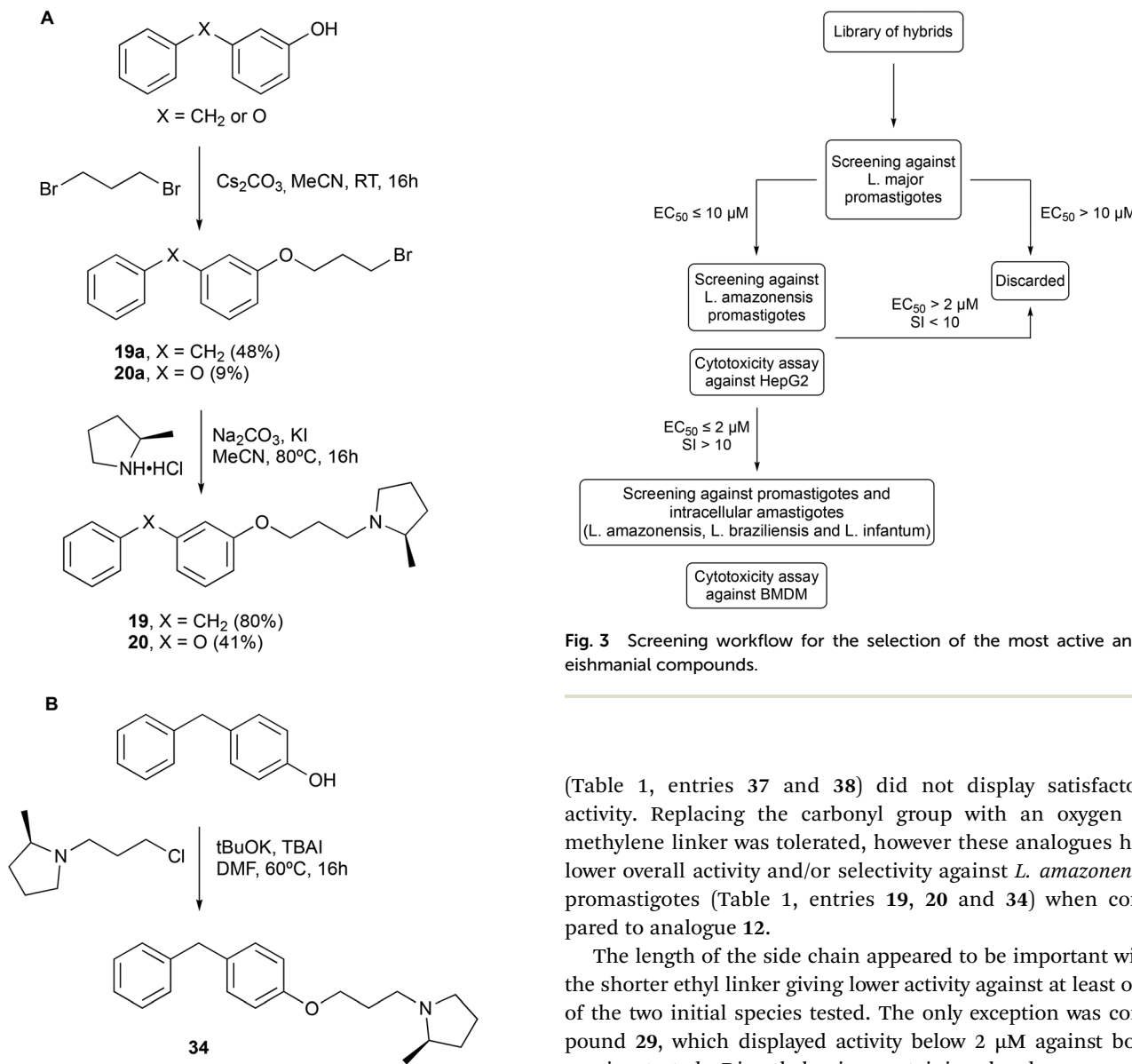
Scheme 2 Synthesis of analogues 35 and 36. (a) K_2CO_3 , TEBA-Cl, EtOAc; (b) K_2CO_3 , MeCN.

(Fig. 3). Using the well-established resazurin cell viability assay,³¹ all compounds were initially screened against *L. major* promastigotes, an Old World CL-causing species. Compounds

exhibiting an $EC_{50} < 10 \mu M$ were selected for further screening against *L. amazonensis* as a representative New World CL-causing species. In this step, compounds were also assayed against HepG2 cells to assess their cytotoxicity to mammalian cells (Table 1). The most active compounds that displayed an $EC_{50} \leq 2 \mu M$ against both *Leishmania* species as well as a selectivity index (SI) above 10 were singled out for further characterisation (Fig. 4). This included assays against promastigotes of *L. braziliensis* and *L. infantum*, causative agents of CL and VL in South America, respectively, as well as anti-intracellular amastigote assays against *L. amazonensis* and *L. infantum*. Additionally, these compounds were assayed against bone-marrow derived macrophages (BMDM), a host cell considered as model of infection for drug susceptibilities studies in *Leishmania*.³²

The screenings against promastigotes of *L. major* and *L. amazonensis* allowed for insights regarding the structure-activity relationship (SAR) of these compounds. Firstly, there was a notable difference in activity dependent on the position of the aminoalkoxy side chain on ring B in relation to the central ketone. Compounds with a *meta*-arrangement (Table 1, entries 11–16) were the most active with 15 and 16, for example, having an $EC_{50} \leq 1 \mu M$ against both species tested as well as a promising selectivity index. In contrast, the set of *ortho*-substituted analogues contained the least active com-





Scheme 3 Synthesis of analogues: (A) 19 and 20; (B) 34.

pounds (Table 1, entries 1–10), and the *para*-substituted group showed intermediate activity (Table 1, entries 23–33). The presence of a chlorine substituent in either ring A (*ortho*-substituted analogues) or ring B (*meta*- and *para*-substituted analogues) resulted in enhanced activity. Although the *para*- and *meta*-chloro substituents were equally effective, the first is a more chemically accessible position and was chosen for further studies. Replacing the chlorine atom by a methyl group is tolerated, however a bulkier substituent such as the isopropyl group caused loss in activity and increased cytotoxicity. The mono-aromatic analogues tested were inactive against both promastigote species, rendering the diaryl system essential for activity (Table 1, entries 35 and 36). Benzophenones with a benzylic aminoalkoxy side chain

(Table 1, entries 37 and 38) did not display satisfactory activity. Replacing the carbonyl group with an oxygen or methylene linker was tolerated, however these analogues had lower overall activity and/or selectivity against *L. amazonensis* promastigotes (Table 1, entries 19, 20 and 34) when compared to analogue 12.

The length of the side chain appeared to be important with the shorter ethyl linker giving lower activity against at least one of the two initial species tested. The only exception was compound 29, which displayed activity below 2 μM against both species tested. Dimethylamine-containing headgroups were also less active when compared to the pyrrolidine-containing compounds. For the latter, the *R*-stereoisomer (Table 1, entry 12) was approximately four-fold more effective than the *S*-enantiomer (Table 1, entry 21) against *L. amazonensis*. Consistent with this, the *gem* dimethyl analogue (Table 1, entry 22) was examined and found to be equipotent with the *R* isomer, but as this precursor amine is less readily available this was not explored further.

Finally, the seven most active compounds (12, 15–17, 20, 29 and 30) were then further characterised for activity against promastigotes of *L. braziliensis* and *L. infantum* (Table 2) and intracellular amastigotes of *L. amazonensis* and *L. infantum*, following cytotoxicity evaluation in BMDM (Table 3). These analyses indicated that these chimeric compounds show high efficacy and selectivity against all four species tested. Additionally, good levels of activity were observed in the intramacrophage amastigote assay, with four compounds (16, 17, 20 and 29) displaying an $EC_{50} \leq 2 \mu\text{M}$ and a $SI > 10$. Overall, when compared

Table 1 Activity of tamoxifen/clemastine hybrid molecules against promastigotes of *L. major* and *L. amazonensis* and cytotoxicity in HepG2 cells

Compounds	Scaffold	X	Y	Carbon chain	R	EC ₅₀ <i>L. major</i> ^a	EC ₅₀ <i>L. amazonensis</i> ^a	CC ₅₀ HepG2 ^a	SI (<i>L. major</i>) ^b	SI (<i>L. amazonensis</i>) ^b
1	A	H	—	2	F	>100	ND	ND	ND	ND
2	A	H	—	3	F	32.51 ± 5.77	ND	ND	ND	ND
3	A	Cl	—	2	F	68.91 ± 15.92	ND	ND	ND	ND
4	A	Cl	—	3	F	11.76 ± 1.1	ND	ND	ND	ND
5	A	H	—	2	G	45.93 ± 15.68	ND	ND	ND	ND
6	A	H	—	3	G	30.11 ± 9.04	ND	ND	ND	ND
7	A	H	—	4	G	11.14 ± 0.23	ND	ND	ND	ND
8	A	Cl	—	2	G	35.78 ± 5.5	ND	ND	ND	ND
9	A	Cl	—	3	G	18.53 ± 3.24	ND	ND	ND	ND
10	A	Cl	—	4	G	1.62 ± 1.48	3.07 ± 0.92	>100	>61	>32
11	B	H	C=O	2	G	4.58 ± 1.65	>100	>100	>22	—
12	B	H	C=O	3	G	1.4 ± 0.0025	0.74 ± 0.13	>100	>71	>135
13	B	H	C=O	4	G	0.93 ± 0.16	3.51 ± 1.44	>100	>107	>48
14	B	Cl	C=O	2	G	5.14 ± 2.71	24.8 ± 10.51	>100	>19	>4
15	B	Cl	C=O	3	G	0.27 ± 0.026	0.37 ± 0.14	>100	>370	>270
16	B	Cl	C=O	4	G	0.30 ± 0.065	0.85 ± 0.46	25.64 ± 0.94	85	30
17	B	Methyl	C=O	3	G	0.63 ± 0.17	1.44 ± 0.44	>100	>158	>69
18	B	Isopropyl	C=O	3	G	5.35 ± 1.04	8.49 ± 2.64	16.45 ± 3.99	3	2
19	B	H	CH ₂	3	G	0.85 ± 0.23	3.07 ± 0.19	>100	>117	>32
20	B	H	O	3	G	1.33 ± 0.3	1.77 ± 0.30	22.71 ± 3.50	17.07	12.83
21	B	H	C=O	3	G ^c	ND	3.03 ± 0.43	ND	ND	ND
22	B	H	C=O	3	G ^d	ND	0.62 ± 0.063	ND	ND	ND
23	C	H	C=O	2	F	11.61 ± 2.68	ND	ND	ND	ND
24	C	H	C=O	3	F	7.07 ± 1.4	4.69 ± 1.38	ND	ND	ND
25	C	H	C=O	4	F	2.91 ± 0.26	1.58 ± 0.25	>100	>34	>63
26	C	H	C=O	2	G	4.51 ± 0.35	1.2 ± 0.35	>100	>22	>83
27	C	H	C=O	3	G	4.25 ± 0.12	3.69 ± 1.51	>100	>23	>27
28	C	H	C=O	4	G	5.37 ± 0.42	2.56 ± 0.84	>100	>18	>39
29	C	p-Cl	C=O	2	G	2.02 ± 0.005	0.8 ± 0.27	>100	>49	>125
30	C	p-Cl	C=O	3	G	2.37 ± 0.18	1.56 ± 0.59	31.07 ± 11.04	13	19
31	C	p-Cl	C=O	4	G	2.2 ± 0.56	1.42 ± 0.52	16.05 ± 2.13	7	11
32	C	m-Cl	C=O	3	G	2.96 ± 0.4	1.14 ± 0.39	25.11 ± 2.03	8	22
33	C	o-Cl	C=O	3	G	0.63 ± 0.001	6.77 ± 0.93	>100	>158	>15
34	C	H	CH ₂	3	G	0.62 ± 0.3	7.25 ± 0.61	27.06 ± 6.67	44	3.73
35	D	MeC=O	—	3	G	>100	>100	>100	ND	ND
36	D	H	—	3	G	>100	>100	>100	ND	ND
37	E	—	—	2	F	8.01 ± 2.39	10.27 ± 2.9	ND	ND	ND
38	E	—	—	3	F	>10	>10	ND	ND	ND
Clemastine	—	—	—	—	—	0.035 ± 0.012	0.038 ± 0.003	25.57 ± 1.76	730	673
Tamoxifen	—	—	—	—	—	4.03 ± 0.33	2.39 ± 0.17	31.32 ± 1.91	8	13
Miltefosine	—	—	—	—	—	6.57 ± 0.89	20.71 ± 3.54	ND	ND	ND

^a Values represent the average and standard error of the mean in micromolar (μM) of three independent experiments in triplicate. ^b The SI (selectivity index) was determined as the ratio between the CC₅₀ of HepG2 cells and EC₅₀ of promastigotes of the indicated *Leishmania* species.

^c G-head groups is (2S)-methylpyrrolidine stereoisomer. ^d G-head groups is 2,2-dimethylpyrrolidine. ND, data not determined.

with both clemastine and tamoxifen, these hybrids exhibit intermediary activity against *L. major* and *L. amazonensis* and in the case of analogues **15** and **16** comparable activity to clemastine against *L. braziliensis* and *L. infantum*. As with clemas-

tine, the hybrids have a significantly lower sp² atom count and a higher degree of flexibility than tamoxifen, which may contribute to this higher activity. However, whilst more active, the synthesis of clemastine is non-trivial, challenging further



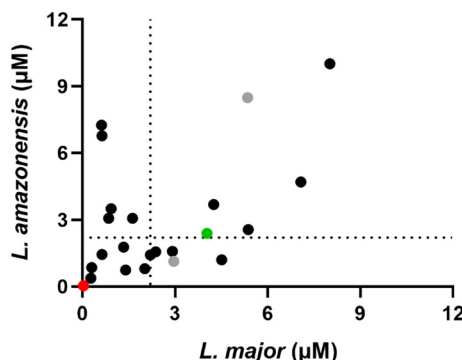


Fig. 4 Relative activity of compounds against *L. major* and *L. amazonensis* promastigotes. Dots represent compounds with an $EC_{50} \leq 10 \mu\text{M}$ for both species. Red dot is clemastine fumarate; green dot is tamoxifen; grey dots are compounds with $SI < 10$ for at least one species. Dotted line is the $2 \mu\text{M}$ cut-off for selection of compounds with highest activity, where compounds within the bottom left quadrant were selected. Data are the average EC_{50} values (in μM) of three independent experiments.

structural variations. The short and simple synthetic route to the hybrids renders these structures as highly promising templates for further lead optimisation.

3. Conclusions

The standard cut off values suggested by the Drugs for Neglected Diseases initiative (DNDi) for lead discovery programs for antileishmanials is an $EC_{50} \leq 2 \mu\text{M}$ against both intracellular amastigotes and promastigotes as well as a selectivity index (SI) above 10.³³ Importantly for the development of new antileishmanial drugs, the results obtained demonstrate that this benchmark has been met across a range of parasite species of both Old and New World origin, and suggest that these easy-to-synthesise chimeric structures therefore represent versatile starting points for a lead optimisation programme. The success of this simple phenotypic driven fragment linking strategy suggest that this may be a productive method for the development of other promising compounds. As with many anti-leishmanials, including all the existing approved drugs, although both clemastine fumarate and tamoxifen target IPCS they also exhibit polypharmacology with other modes of action.^{19,34} It is likely that these hybrids retain these characteristics, and these different activities will be impacted in different ways by the structural changes made which may account for the variable levels of activity observed. It is possible to speculate that the more consistent level of activity exhibited by **15** and **16** across a range of *Leishmania*

Table 2 Activity of the most promising compounds against promastigotes of *L. braziliensis* and *L. infantum*

Compounds	EC_{50}^a <i>L. braziliensis</i>	EC_{50}^a <i>L. infantum</i>	SI^b (<i>L. braziliensis</i>)	SI^b (<i>L. infantum</i>)
12	0.53 ± 0.14	4.42 ± 0.27	>189	>23
15	0.38 ± 0.054	1.32 ± 0.12	>263	>76
16	0.21 ± 0.044	1.00 ± 0.14	124	26
17	0.65 ± 0.12	2.93 ± 0.11	>154	>34
20	0.26 ± 0.10	2.84 ± 0.16	88	8
29	0.41 ± 0.091	2.32 ± 0.091	>243	>43
30	0.084 ± 0.015	1.25 ± 0.11	369	25
Clemastine	0.14 ± 0.002	0.71 ± 0.043	186	36
Tamoxifen	9.55 ± 2.045	4.97 ± 0.49	3	6

^aValues represent the average and standard error of the mean in micromolar (μM) of three independent experiments in triplicate. ^bThe SI (selectivity index) was determined as the ratio between the CC_{50} of HepG2 cells and EC_{50} of promastigotes of the indicated *Leishmania* species.

Table 3 Activity of the most promising compounds against intracellular amastigotes of *L. amazonensis* and *L. infantum*, and cytotoxicity evaluation in BMDM

Compounds	CC_{50}^a BMDM	EC_{50}^a <i>L. amazonensis</i>	EC_{50}^a <i>L. infantum</i>	SI^b (<i>L. amazonensis</i>)	SI^b (<i>L. infantum</i>)
12	>100	3.95 ± 0.38	1.30 ± 0.35	25	77
15	36.38 ± 6.25	5.35 ± 1.055	0.69 ± 0.18	7	53
16	32.48 ± 5.01	2.11 ± 0.43	2.43 ± 0.58	15	13
17	48.73 ± 9.77	2.44 ± 0.59	1.19 ± 0.29	20	41
20	49.46 ± 0.36	0.80 ± 0.096	1.076 ± 0.14	62	46
29	>100	2.27 ± 0.26	1.72 ± 0.44	44	58
30	43.13 ± 2.30	3.89 ± 0.70	0.86 ± 0.17	11	50
Clemastine	22.35 ± 3.78	0.46 ± 0.10	ND	49	ND
Tamoxifen	52.44 ± 2.34	4.90 ± 0.69	2.4 ± 0.3	10	22

^aValues represent the average and standard error of the mean in micromolar (μM) of three independent experiments in triplicate. ^bThe SI (selectivity index) was determined by the ratio between the CC_{50} of BMDM and EC_{50} of promastigotes of the indicated *Leishmania* species. ND, data not determined.



species may indicate a more focused mode of action. A better understanding of the target(s) and mechanisms of action of both these compounds and the parent drug and is needed to clarify this and direct further studies. The easier access to these hybrids facilitates such studies and work towards target identification is ongoing and will be described in due course.

4. Experimental

4.1. Chemical synthesis

4.1.1. General conditions. IR spectra were acquired using a PerkinElmer Spectrum 1000 FT-IR spectrometer equipped with an ATR module, and absorption maxima ν_{max} were reported as wavenumbers (cm^{-1}). Nuclear Magnetic Resonance (NMR) spectra were acquired on Varian VNMRS 700 (^1H at 700 MHz, ^{13}C at 176 MHz) or Varian VNMRS 600 (^1H at 600 MHz, ^{13}C at 151 MHz). Chemical shifts are reported in ppm (δ). High resolution mass spectra (HRMS) were obtained using Waters LCT Premier XE with an electrospray ionization (ESI) source. Unless otherwise mentioned, reactions were performed under an inert nitrogen atmosphere. Spectroscopic and analytical characterisation, as well as the detailed synthesis for all compounds can be found in the ESI.† All compounds explored in the biological assays were of >95% purity as ascertained by $^1\text{H}/^{13}\text{C}$ NMR and LCMS analysis.

4.1.2. General procedure for $\text{S}_{\text{N}}2$ reactions. Cs_2CO_3 was added to a solution of hydroxybenzophenone in anhydrous DMF or MeCN, and the resulting suspension stirred at RT for 30 min. The dibromoalkyl was added and the solution stirred at RT for 16 h. In case a dimethylaminoalkyl chloride was used, the solution stirred under reflux. The reaction mixture was diluted in water and extracted with EtOAc. The combined organic extracts were washed with brine, dried over MgSO_4 , and concentrated under reduced pressure. The final compounds containing the dimethylamine head group were submitted to purification by column chromatography (10% MeOH in DCM), whilst the bromide-containing electrophiles were used without further purification. The crude product was dissolved in either anhydrous DMF or MeCN, together with TBAI and (2*R*)-methylpyrrolidine hydrochloride. The reaction stirred at reflux for 16 h and was cooled down to room temperature before dilution with sat. Na_2CO_3 (aq). The products were extracted with EtOAc and combined organic layers were washed once with sat. Na_2CO_3 (aq), dried over MgSO_4 , filtered, and concentrated *in vacuo* before being submitted to column chromatography (10% MeOH in DCM).

4.2. *Leishmania* culture

Leishmania amazonensis (MHOM/BR/1975/JOSEFA), *Leishmania major* (MHOM/IL/80/Friedlin), *Leishmania braziliensis* (MHOM/BR/1994/H3227) and *Leishmania infantum* (MHOM/BR/1972/LD) were cultivated at 25 °C in Schneider's insect medium at pH 7, supplemented with 15% heat-inactivated fetal bovine serum (FBS) and penicillin/streptomycin 100 $\mu\text{g mL}^{-1}$. Transgenic lines of *L. amazonensis* and *L. infantum* expressing

luciferase were previously generated, maintained in media containing 32 $\mu\text{g mL}^{-1}$ hygromycin B^{35,36} and used for anti-amas-tigote dose-response assays (item 4.6).

4.3. HepG2 cell culture

HepG2 cells were cultivated at 37 °C in a 5% CO_2 atmosphere in DMEM supplemented with 10% FBS, containing 100 $\mu\text{g mL}^{-1}$ penicillin/streptomycin. Cells were split every 3 days by removing the media and adding trypsin, which were then incubated for 10 min at 37 °C in a 5% CO_2 atmosphere. Trypsin was deactivated by adding 20 mL fresh media, which was homogenised and added to a new culture flask in a 1:4 proportion.

4.4. Anti-promastigote dose-response assay

Log-phase promastigotes were quantified and suspended in fresh medium to a density of 1×10^6 parasites per ml. In a 96-well plate, 1×10^5 parasites were applied per well and parasites were incubated at 25 °C in increasing concentrations of each compound for 44 hours. Then, 10 μL of 0.1 mg mL^{-1} resazurin solution (Fisher Scientific, Leicestershire, UK) were added per well and the plate was incubated for 4 hours at 25 °C. Fluorescence (excitation at 555 nm and emission at 585 nm) was detected using the PolarStar Omega luminometer (BMGLabTech). EC₅₀ values were obtained by GraphPad Prism 6, after determination of sigmoidal regression curves. At least three independent experiments in triplicates were performed for each molecule. Tamoxifen and clemastine were used as control drugs.

4.5. Cytotoxicity assays

HepG2 cells were detached when cell culture was approximately 80% confluent and quantified to be resuspended in fresh DMEM medium to a density of 5×10^4 cells per mL which 200 μL were added to each well (1×10^4 cells) in a 96-well plate incubated overnight at 37 °C in a 5% CO_2 atmosphere. For BMDM, the cells were plated as described in the section 4.6. In both cases, the supernatant was removed and fresh media containing several concentrations of compounds was added, and plates incubated at 37 °C on a 5% CO_2 atmosphere for 44 hours. Next, 10 μL of 0.1 mg mL^{-1} resazurin solution (Fisher Scientific, Leicestershire, UK) were added per well and incubated for 4 h before fluorescence intensity was determined, using a plate reader (excitation at 555 nm and emission at 585 nm). At least three independent experiments were performed for each molecule with all samples in triplicates. Every plate had tamoxifen or clemastine as the control. EC₅₀ values were obtained by GraphPad Prism 6, after determination of sigmoidal regression curves.

4.6. Anti-intramacrophage amastigote dose-response assay

Bone-marrow-derived macrophages (BMDM) were obtained from female BALB/c mice, which were cultivated in RPMI 1640 medium (Thermo Fisher Scientific) supplemented with 10% FBS, 0.1 M sodium pyruvate, and 100 $\mu\text{g mL}^{-1}$ penicillin/streptomycin and incubated in a 5% CO_2 atmosphere at 37 °C,

as previously described.³⁶ The macrophages were plated in 96-well plates with a density of 8×10^4 cells per well in 100 μL per well. After incubation for 24 hours, the macrophages were infected with stationary-phase promastigotes at a ratio of 20 : 1 (parasites/macrophage) for both *L. amazonensis* and *L. infantum*. After 4 hours of incubation at 34 °C (except for *L. infantum* that was incubated at 37 °C), 200 μL of fresh medium containing several concentrations of the compounds tested was added to the wells, and the plates were incubated for 72 hours at 34 °C or 37 °C for *L. infantum*. Next, 15 μL of luciferin (One-Glo Luciferase Assay System, Promega) were then added per well and bioluminescence was measured in a PolarStar Omega luminometer (BMGLabTech). Parasite survival in treated samples was determined based on the ratio of treated/untreated cells. EC₅₀ values were obtained by GraphPad Prism 6, after determination of sigmoidal regression curves. At least three independent experiments in triplicate were performed for each molecule with all samples.

For experiments using mice, protocols and procedures were approved by the Ethics Committee for Animal Experimentation of the Instituto de Biologia, Universidade Estadual de Campinas (UNICAMP) (protocol: 5719-1/2021). Animals were obtained from Centro Multidisciplinar para Investigação Biológica (CEMIB) of UNICAMP and kept in mini-isolators, receiving food and water ad libitum.

4.7. Statistical analysis

All statistical analyses were performed by GraphPad Prism 6 (CA, USA), using ANOVA *one-way* test and multiple comparisons Dunnett's test. *P* value <0.05 was considered as statistically significant.

Author contributions

PGS and SRBU conceived and designed the project. PGS, PWD and ACC supervised the project. VSA and MBB designed and conducted the experiments and collected the data. VSA, PGS, PWD and ACC analysed the results. VSA and PGS drafted the manuscript. All authors read, reviewed, and approved the final draft.

Conflicts of interest

The authors declare that the research was conducted in the absence of any commercial or financial relationships that could be construed as a potential conflict of interest.

Acknowledgements

We thank Durham University GCRF CDT (studentship to VSA), The Royal Society (The Royal Society International Collaboration Awards for Research Professors 2016: IC160044), the UKRI Global Challenges Research Fund under grant agreement 'A Global Network for Neglected Tropical Diseases'

(grant number MR/P027989/1), and the GCRF and Newton Fund Consolidation Account (GNCA) EP/X527713/1 for financial support. We also thank Camilo C. Janeri for technical assistance with animal-related experiments.

References

- 1 S. Burza, S. L. Croft and M. Boelaert, *Lancet*, 2018, **392**, 951–970.
- 2 S. Mohan, P. Revill, S. Malvolti, M. Malhame, M. Sculpher and P. M. Kaye, *PLoS Neglected Trop. Dis.*, 2022, **16**, 1–17.
- 3 A. Poulaki, E. T. Piperaki and M. Voulgaridis, *Microorganisms*, 2021, **9**, 759.
- 4 T. F. Silva, F. Tomiotti-Pellissier, A. K. S. Pasquali, F. Pinto-Ferreira, W. R. Pavanelli, I. Conchon-Costa, I. T. Navarro and E. T. Caldart, *Acta Trop.*, 2021, **221**, 106018.
- 5 I. Abadías-Granado, A. Diago, P. A. Cerro, A. M. Palma-Ruiz and Y. Gilaberte, *Actas Dermo-Sifiliogr.*, 2021, **112**, 601–618.
- 6 WHO. World Health Organization, *Status of endemicity of cutaneous leishmaniasis*, 2022.
- 7 WHO. World Health Organization, *Status of endemicity of visceral leishmaniasis*, 2022.
- 8 F. Baileyid, K. Mondragon-Shem, L. R. Haines, A. Olabi, A. Alorfi, J. A. Ruiz-Postigo, J. Alvar, P. Hotez, E. R. Adams, I. D. Vélez, W. Al-Salem, J. Eaton, Á. Acosta-Serrano and D. H. Molyneux, *PLoS Neglected Trop. Dis.*, 2019, **13**, 1–22.
- 9 M. Pires, B. Wright, P. M. Kaye, V. da Conceição and R. C. Churchill, *PLoS One*, 2019, **14**, 1–21.
- 10 M. Yanik, M. S. Gurel, Z. Simsek and M. Kati, *Clin. Exp. Dermatol.*, 2004, **29**, 464–467.
- 11 S. R. B. Uliana, C. T. Trinconi and A. C. Coelho, *Parasitology*, 2017, 1–17.
- 12 S. Salari, M. Bamorovat, I. Sharifi and P. G. N. Almani, *J. Clin. Lab. Anal.*, 2022, **36**, 1–16.
- 13 M. O. Harhay, P. L. Olliaro, M. Vaillant, F. Chappuis, M. A. Lima, K. Ritmeijer, C. H. Costa, D. L. Costa, S. Rijal, S. Sundar and M. Balasegaram, *Am. J. Trop. Med. Hyg.*, 2011, **84**, 543–550.
- 14 D. C. Swinney and J. Anthony, *Nat. Rev. Drug Discovery*, 2011, **10**, 507–519.
- 15 S. Pushpakom, F. Iorio, P. A. Evers, K. J. Escott, S. Hopper, A. Wells, A. Doig, T. Guilliams, J. Latimer, C. McNamee, A. Norris, P. Sanseau, D. Cavalla and M. Pirmohamed, *Nat. Rev. Drug Discovery*, 2018, **18**, 41–58.
- 16 S. S. Braga, *Eur. J. Med. Chem.*, 2019, 183.
- 17 D. C. Miguel, J. K. U. Yokoyama-Yasunaka, W. K. Andreoli, R. A. Mortara and S. R. B. Uliana, *J. Antimicrob. Chemother.*, 2007, **60**, 526–534.
- 18 C. T. Trinconi, J. Q. Reimão, V. I. Bonano, C. R. Espada, D. C. Miguel, J. K. U. Yokoyama-Yasunaka and S. R. B. Uliana, *Parasitology*, 2018, **145**, 490–496.
- 19 J. G. M. Mina, R. L. Charlton, E. Alpizar-Sosa, D. O. Escrivani, C. Brown, A. Alqaisi, M. P. G. Borsodi, C. P. Figueiredo, E. V. De Lima, E. A. Dickie, W. Wei,



R. Coutinho-Silva, A. Merritt, T. K. Smith, M. P. Barrett, B. Rossi-Bergmann, P. W. Denny and P. G. Steel, *ACS Infect. Dis.*, 2021, **7**, 47–63.

20 A. Munshi and P. Singh, *Breast*, 2008, **17**, 121–124.

21 M. N. Singh, H. F. Stringfellow, E. Paraskevaidis, P. L. Martin-Hirsch and F. L. Martin, *Cancer Treat. Rev.*, 2007, **33**, 91–100.

22 D. C. Miguel, J. K. U. Yokoyama-Yasunaka and S. R. B. Uliana, *PLoS Neglected Trop. Dis.*, 2008, **2**, e249.

23 D. C. Miguel, R. C. Zauli-Nascimento, J. K. U. Yokoyama-Yasunaka, S. Katz, C. L. Barbiéri and S. R. B. Uliana, *J. Antimicrob. Chemother.*, 2009, **63**, 365–368.

24 C. T. Trinconi, J. Q. Reimão, J. K. U. Yokoyama-Yasunaka, D. C. Miguel and S. R. B. Uliana, *Antimicrob. Agents Chemother.*, 2014, **58**, 2608–2613.

25 C. T. Trinconi, J. Q. Reimão, A. C. Coelho and S. R. B. Uliana, *J. Antimicrob. Chemother.*, 2016, **71**, 1314–1322.

26 H. B. Kaiser, *J. Allergy Clin. Immunol.*, 1990, **86**, 1000–1003.

27 C. T. Trinconi, D. C. Miguel, A. M. Silber, C. Brown, J. G. M. Mina, P. W. Denny, N. Heise and S. R. B. Uliana, *Int. J. Parasitol.: Drugs Drug Resist.*, 2018, **8**, 475–487.

28 K. M. Kasiotis and S. A. Haroutounian, *Curr. Org. Chem.*, 2012, **16**, 335–352.

29 A. M. Fournier, R. A. Brown, W. Farnaby, H. Miyatake-Ondozabal and J. Clayden, *Org. Lett.*, 2010, **12**, 2222–2225.

30 P. Steel, P. Denny, R. Charlton and B. Rossi-Bergmann, WO application No. WO2023047107A1, 2022.

31 A. Kulshrestha, V. Bhandari, R. Mukhopadhyay, V. Ramesh, S. Sundar, L. Maes, J. C. Dujardin, S. Roy and P. Salotra, *Parasitol. Res.*, 2013, **112**, 825–828.

32 R. C. Zauli-Nascimento, D. C. Miguel, J. K. U. Yokoyama-Yasunaka, L. I. A. Pereira, M. A. Pelli De Oliveira, F. Ribeiro-Dias, M. L. Dorta and S. R. B. Uliana, *Trop. Med. Int. Health*, 2010, **15**, 68–76.

33 K. Katsuno, J. N. Burrows, K. Duncan, R. H. Van Huijsdijnen, T. Kaneko, K. Kita, C. E. Mowbray, D. Schmatz, P. Warner and B. T. Slingsby, *Nat. Rev. Drug Discovery*, 2015, **14**, 751–758.

34 C. T. Trinconi, D. C. Miguel, A. M. Silber, C. Brown, J. G. M. Mina, P. W. Denny, N. Heise and S. R. B. Uliana, *Int. J. Parasitol.: Drugs Drug Resist.*, 2018, **8**, 475–487.

35 J. Q. Reimão, C. T. Trinconi, J. K. Yokoyama-Yasunaka, D. C. Miguel, S. P. Kalil and S. R. B. Uliana, *J. Microbiol. Methods*, 2013, **93**, 95–101.

36 J. Q. Reimão, J. C. Oliveira, C. T. Trinconi, P. C. Cotrim, A. C. Coelho and S. R. B. Uliana, *PLoS Neglected Trop. Dis.*, 2015, **9**, e0003556.

